RSC Advances

RSC Advances

www.rsc.org/advances

ROYAL SOCIETY
OF CHEMISTRY

www.rsc.org/advances

RSC Advances

PAPER

Mechanochemical Synthesis of Efficient Nanocrystalline BaFBr:Eu^{2+} X-ray Storage Phosphor

Xianglei Wang and Hans Riesen*

A straightforward and direct preparation route for nanocrystalline BaFBr:Eu^{2+} by ball-milling is reported. We demonstrate that the as-prepared nanocrystalline powder becomes an efficient photostimulable x-ray storage phosphor upon annealing at temperatures in the range of 400 to 900 ^{o}C. The dependence of crystallite size, photoluminescence and storage phosphor properties on annealing temperature and annealing time was investigated and the optimal conditions were determined. After annealing at 900 ^{o}C for 1 h, the average crystallite size was found to be ~200 nm; in comparison with the typical ~5 μm crystallites for conventional phosphors. The shape and size distribution of the particles may allow higher packing densities, resulting in higher sensitivities, and resolution in computed radiography. The photostimulable storage properties compare favorably with results obtained for a commercial BaFBr(I):Eu^{2+} imaging plate.

1 Introduction

BaFBr$_{1-x}$I$_x$ (x=0 to 0.05) doped with divalent europium has been the most widely used and successful x-ray storage phosphor in computed radiography to date and was investigated by the Fuji Film Company as early as the 1980s.[1-3] The readout mechanism of this storage phosphor employs photostimulated luminescence, which has been extensively reviewed in the literature.[4-7] The storage mechanism is based on the generation of electron-hole pairs upon x-irradiation with subsequent trapping at two centres. In BaFBr:Eu^{2+}, F$^+$-centres (halide vacancies) act as electron traps upon x-irradiation and the electrons can be released by subsequent photostimulation from these traps. There are two types of F-centres: F(Br$^-$) and F(F$^-$), but there appears to be some disagreement whether both types are involved.[4,5] There has also been some controversy about the hole trap centres and their role in the photostimulation process. Takahashi et al.[2] considered Eu^{2+} as the hole trap and reported a mechanism that results in the ionization of Eu^{2+} to Eu^{3+}. Upon subsequent photostimulation Eu^{3+} centres are then thought to trap the electrons released from the F-centres, yielding excited Eu^{2+} activators that relax to the ground state and emit the broad band 4f^{6}5d-4f^7 luminescence around 390 nm. However, other researchers reported that no Eu^{3+} can be observed in their experiments.[8-10] For example, von Seggern et al.[4] and Meijerink et al.[9] could not observe any reduction or increase of Eu^{2+} or Eu^{3+} luminescence, respectively, as a function of x-irradiation. Based on EPR measurements Hangleiter et al.[8] proposed a mechanism that involves a spatial correlation of isolated F

centres and hole centres. In particular, it was suggested that aggregates of Eu^{2+} with F centres, aggregates of Eu^{2+} with hole centres, and a low concentration of aggregates of Eu^{2+} with both F and hole centres were formed upon x-ray irradiation. It was also found that O^{2-} ions, an ubiquitous impurity in BaFX (X=Cl, Br) compounds, can act as hole trap centres.[11,12] Notwithstanding the vast number of investigations into BaFBr:Eu^{2+} as an x-ray storage phosphor, some details of the mechanism for photostimulated luminescence are still not fully understood and warrant further investigations.

BaFBr(I):Eu^{2+} was initially, and typically still is, synthesized by high temperature sintering of stoichiometric mixtures of the solid reagents under an inert atmosphere.[1-3] Various methods have been reported in the literature thereafter, such as non-stoichiometric sintering[13-15] and co-precipitation of water based solutions.[16] Recently, von Seggern et al.[17] introduced a single step synthesis method by annealing BaCO$_3$ and ammonium halides with trace amounts of EuF$_3$ in a reducing atmosphere. They investigated the correlation between the intensity of photoluminescence and photostimulated luminescence with the annealing temperature and reported that the optimal particle size for microcrystalline BaFBr:Eu^{2+} is about 5 μm after annealing at 800 ^{o}C.

Recently, a one-step ball-milling method was reported for preparing nanocrystalline BaFCl:Sm^{3+},[18] BaFCl:Sm^{2+},[19] and Ba$_{0.5}$Sr$_{0.5}$FCl$_{0.5}$Br$_{0.5}$:Sm^{3+}.[20] In the present paper, a similar method was applied for the preparation of nanocrystalline BaFBr:Eu^{2+} and the as-prepared sample was annealed up to 900 ^{o}C to investigate its properties as a potentially improved x-ray storage phosphor.

2 EXPERIMENTAL

School of Physical, Environmental and Mathematical Sciences, The University of New South Wales, Canberra, ACT 2600, Australia. E-mail: h.riesen@adfa.edu.au

Reagents obtained from Sigma-Aldrich Pty Ltd. were used without further purification. First, 0.877g (5 mmol) barium fluoride (BaF_2, 99.99% trace metals basis) was ground and dried under vacuum at 400 °C for 3 h. Then 1.486g (5 mmol) anhydrous barium bromide ($BaBr_2$, beads, 99.999% trace metals basis, in ampoule), 0.048 mmol europium bromide ($EuBr_2$, 99.99% trace metals basis; 1 weight-% of $BaBr_2$) and the vacuum dried BaF_2 were mixed and ground in a nitrogen purged glove box to avoid oxidation of the Eu^{2+} ions. The mixture was subsequently placed into a 10 mL zirconia jar with two 12 mm diameter zirconia balls under nitrogen and the jar was sealed with parafilm. The solid reagents were then ball-milled on a Retsch Mixer Mill 200 at a frequency of 20 Hz for 120 min to yield nanocrystalline $BaFBr:Eu^{2+}$ as a white powder. Subsequently, the as-prepared nanocrystalline $BaFBr:Eu^{2+}$ was annealed in separate batches under vacuum for 1 h at temperatures between 150 °C and 900 °C; it is noted here that the latter is just ~80 °C below the melting temperature of $BaFBr$.[21] In a second experiment, separate batches of the sample were also annealed under vacuum at 900 °C for different time periods between 1 to 6 h.

From an analysis by employing an energy dispersive x-ray fluorescence spectrometer (Shimadzu EDX-800HS), we found that the samples prepared by the ball-milling method were only very slightly contaminated by zirconia (from the jar and balls) at an insignificant level of <0.03 weight-% .

The powder x-ray diffraction (XRD) patterns of the samples were measured using a Rigaku MiniFlex 600 benchtop diffractometer operating at 40 kV and 15 mA with CuK_α radiation (λ=0.154 nm). All data were collected at room temperature in a step-scanning mode with a speed of 0.75 °/min and a 2-theta range from 10° to 90°. The measured XRD patterns were compared with the standard reference data ICDD card 24-90.

Scanning electron microscopy (SEM) was conducted on a JEOL 7001 Field Emission Scanning Electron Microscope. Each samples was dispersed in acetone in an ultrasonic bath and then dropped onto a silicon wafer. The samples were all coated with 10 nm of Pt to make the samples conductive.

Photoluminescence (PL) spectra were measured on a Horiba Jobin-Yvon Spex Fluoromax-3 fluorometer. The excitation wavelength was set to 270 nm, and the spectra were collected in single scans with 0.5 nm steps and 0.5 s integration time.

The 270-nm wavelength is well within a main absorption feature of Eu^{2+} in the BaFBr host and also efficiently excites Eu^{3+} via an O^{2-}- Eu^{3+} charge transfer transition. It is safe to assume that any Eu^{3+} is due to the unintentional contamination of the system with oxygen i.e. oxide defects.

The photostimulated luminescence (PSL) spectra were accumulated on a Spex 500M monochromator equipped with an Andor iDus Model DV401A-BV CCD camera and a Thorlabs FES0500 short pass interference filter was used at the entrance slit. In a typical experiment, the sample was firstly x-irradiated by a Sirona HELIODENT Plus dental system with an exposure time of 3.2 s corresponding to about ~30 mGy entry

surface dose. The x-irradiated sample was then immediately stimulated for 10 s by a red LED (634 nm; ~5 mW/cm²) to measure its photostimulated luminescence spectrum. The photostimulated luminescence intensities of the as-prepared and annealed samples were compared with results obtained for a commercial dental imaging plate (Duerr Dental), which was x-irradiated using the same dental x-ray source with an exposure time of 0.32 s (~3 mGy surface dose). A ten times higher dose was chosen for our samples in order to allow monitoring the weak photostimulated luminescence after annealing at temperatures <400°C.

3 RESULTS AND DISCUSSION

The powder x-ray diffraction patterns of the as-prepared and annealed nanocrystalline $BaFBr:Eu^{2+}$ phosphors are shown in Fig. 1. Prominent peaks in all the patterns could be indexed to the pure PbFCl tetragonal matlockite structure with space group P4/*nmm*.[22] The XRD patterns confirm the purity of the BaFBr phase in the as-prepared and annealed samples. Prominent diffraction peaks become narrower and more intense with higher annealing temperature. From a Williamson-Hall analysis[23] of the prominent peaks, and using a Gaussian line shape approximation, the average crystallite size of the as-prepared sample was estimated to be around 30 nm. This is good agreement with the average particle size as observed in the SEM image shown in Fig. 2a. As is seen in Fig. 1, the (002) peak shows a significantly increased intensity compared to the expected ICDD pattern. This is likely due to preferential orientation of the particles/crystallites with increasing size on the XRD holder.
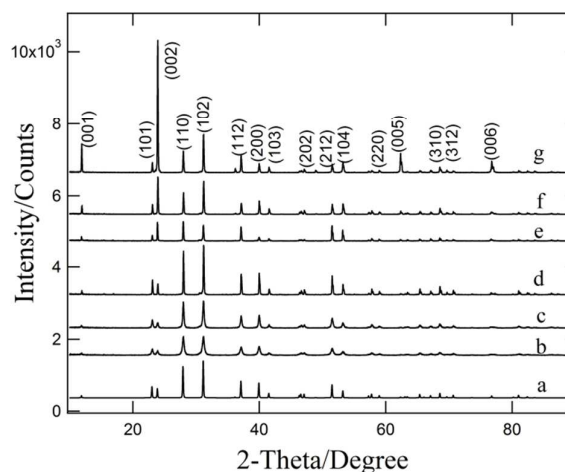

Fig. 1 Powder x-ray diffraction patterns of (a) the standard BaFBr data (ICDD card No. 24-90) and (b) the as-prepared nanocrystalline BaFBr:Eu²⁺, (c) after annealing for 1 h at 300 °C, (d) 600 °C and (e) at 900 °C for 1 h, (f) 3 h and (g) 6 h. Miller-indices are indicated for the prominent peaks.

The crystallite size appears to grow quadratically (T^2) with annealing temperature as is illustrated in the inset of Fig. 4,

reaching a size of about 200 nm after annealing at 900 °C for 1 h. The SEM image displayed in Fig. 2b is commensurate with this result from XRD. Individual batches of the phosphor were also annealed separately at 900 °C for different periods between 1 to 6 h to investigate the effect of annealing time. With prolonged annealing time, the crystallites are sintered/fused into larger aggregates. Whilst after 3 h annealing at 900 °C the average particles are still submicron with crystallites on the 200-300 nm scale (see Fig. 2c), particles on the order of about 5 µm were observed after 6 h annealing.
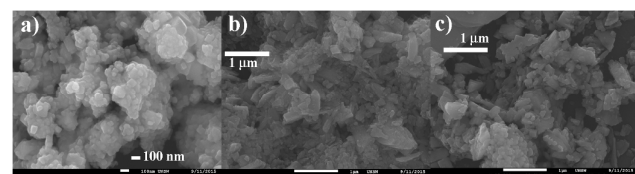

Fig. 2 SEM images of BaFBr:Eu²⁺ as-prepared (a), after subsequent annealing for 1 h (b) and 3 h (c) at 900 °C. Bars are indicating the resolution.

However, these particles consist of fused crystallites that are still mostly on submicron scale.

The photoluminescence spectrum of the as-prepared nanocrystalline BaFBr:Eu²⁺ is shown in Fig. 3. The intense broad-band emission centered at 390 nm is due to the $4f^65d \rightarrow 4f^7$ Eu²⁺ transition. There are also some weak peaks observed in the longer wavelength range due to the ^5D_J-^7F_J Eu³⁺ transitions,[24] most probably a result of oxidation during the storage of chemicals and the ball-milling process. As indicated in the Experimental section, this oxidation is most likely due to the contamination with oxygen, yielding oxide ions that result in a strong O^{2-} - Eu²⁺ charge-transfer excitation around 270 nm.
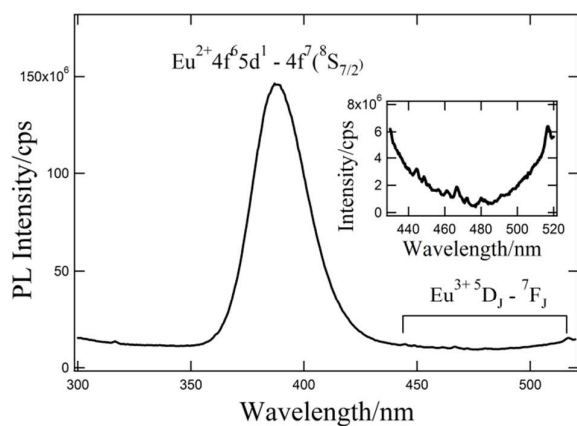

Fig. 3 Photoluminescence spectrum at 298 K of the as-prepared nanocrystalline BaFBr:Eu²⁺ excited at 270 nm. The inset shows a magnification in the region of Eu³⁺ transitions.

Importantly, the spectrum clearly demonstrates that europium ions are mainly incorporated into the BaFBr lattice in their divalent state by our ball-milling method and that the Eu²⁺ photoluminescence is not affected by this minor impurity, for example, by excitation energy transfer from the Eu³⁺ to the

Eu²⁺ ions. The photoluminescence spectra of the as-prepared nanocrystalline BaFBr:Eu²⁺ after individually annealing batches for 1 h from 150 °C up to 900 °C are displayed in Fig. 4. The Eu²⁺ transition becomes stronger with annealing temperature, and the integrated photoluminescence intensity of the emission follows a $T^{4.3}$ power law. Thus the photoluminescence is about quadratically dependent on the crystallite size (the latter grows quadratically with annealing temperature). An increase in photoluminescence intensity of the Eu²⁺ fluorescence with increased annealing temperature was previously observed by von Seggern et al.[17] for microcrystalline BaFBr:Eu²⁺ prepared by high-temperature sintering.

However, when the nanocrystalline BaFBr:Eu²⁺ phosphor was annealed at 900 °C for longer periods of time (2-6 h), no further increase of photoluminescence intensity was observed for the Eu²⁺ transition around 390 nm compared to the result after annealing for 1 h.
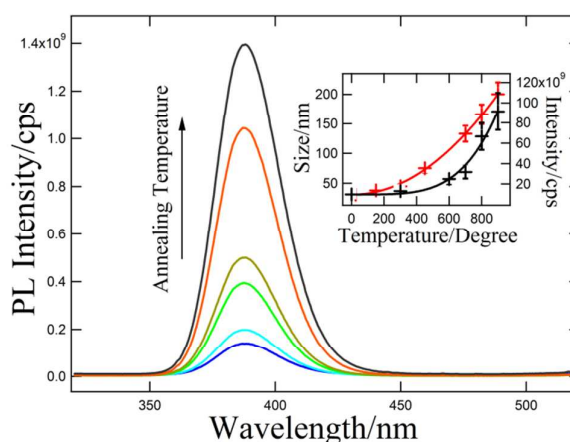

Fig. 4 Photoluminescence spectra at 298 K of nanocrystalline BaFBr:Eu²⁺ excited at 270 nm after annealing for 1 h at (bottom to top) RT, 300, 600, 700, 800, 900 °C. The inset shows the dependence on annealing temperature of the average crystallite size as obtained from XRD (red trace, left axis) and the integrated photoluminescence intensity for the Eu²⁺ transition around 390 nm (black trace, right axis).

The photostimulated luminescence spectra upon x-irradiation for the various nanocrystalline BaFBr:Eu²⁺ samples are shown in Fig. 5 in comparison with the spectrum of a commercial imaging plate. The efficiency of an x-ray storage phosphor can be defined as the number of photostimulated luminescence photons generated per incident x-ray photon.[17] The annealed samples were x-irradiated by the dental x-ray source for 3.2 s, while the commercial plate was x-irradiated for 0.32 s. The two exposures correspond to ~30 and ~3 mGy surface doses, respectively. As shown from Fig. 5, there is very little photostimulated luminescence observed for the as-prepared powder and for samples annealed at temperatures <400 °C. The photostimulated luminescence intensity starts to become significant if the powder is annealed at 400 °C with a dramatic increase with annealing temperature that follows a $T^{5.6}$ power

law. This is in qualitative accord with the observations by von Seggern et al.[17] made for microcrystalline BaFBr:Eu^{2+} prepared by high temperature sintering. According to Ref 17, x-ray induced F-centres are only efficiently generated if samples have been annealed at high temperatures i.e. annealing at high temperatures must create F^{+}-centres (halide vacancies); this appears to cause the dependence of photostimulated luminescence intensity on the annealing temperature. We stress here that the minor variation in the lineshape of the photostimulated spectrum of the commercial imaging plate in comparison with our samples is based on the variation in composition (commercial phosphor contains up to ~5% iodide) and the thin blue filter film that covers the storage phosphor in the commercial plate.

commercial film. Nevertheless, even when we take these factors into account, it follows that the sensitivity is on the same order of magnitude (approximately 5 times less) and it is likely that the slightly higher sensitivity of the commercial phosphor plate is due to the co-doping with iodide ions. Also, the europium concentration in our samples is probably too high leading to self-quenching of the photostimulated emission. The increase in storage efficiency as revealed by a continuing increase of PSL intensity (inset of Fig. 6) is likely due to a continuing creation of F^{+}-centers (halide vacancies) at high temperatures. For the storage phosphor to work efficiently, such centres serve as the electron traps after the electron-hole pair creation upon x-irradiation.
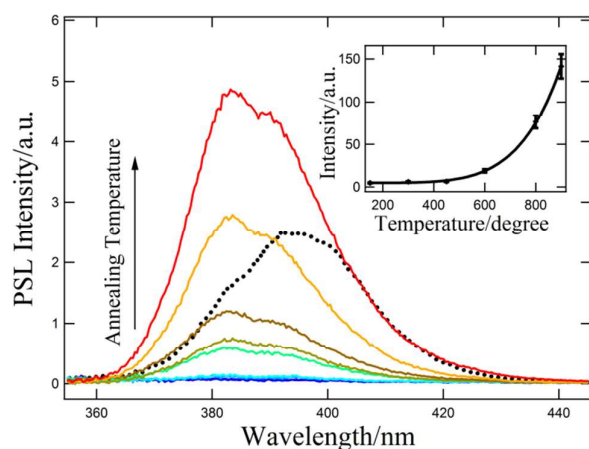

Fig. 5 Photostimulated luminescence spectra at 298 K of nanocrystalline BaFBr:Eu^{2+} as a function of annealing temperature (bottom to top, RT, 150, 300, 450, 600, 800, 900 $^{\circ}$C) compared to the spectrum of a commercial imaging plate (black dotted line). The inset shows the dependence of integrated photostimulated luminescence signal on annealing temperature for the Eu^{2+} transition around 390 nm.
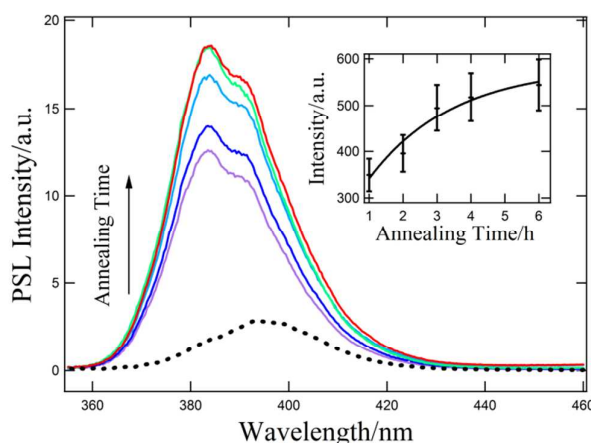

Fig. 6 Photostimulated luminescence spectra at 298 K of nanocrystalline BaFBr:Eu^{2+} after annealing at 900 $^{\circ}$C for 1, 2, 3, 4, 6 h (bottom to top) compared to the spectrum of the commercial imaging plate (black dotted line). The inset shows the dependence of the integrated photostimulated luminescence intensity for the Eu^{2+} transition around 390 nm as a function of annealing time.

4 Conclusions

Photostimulable nanocrystalline BaFBr:Eu^{2+} x-ray storage phosphor was directly prepared by ball milling a mixture of BaF$_2$, BaBr$_2$ and trace of EuBr$_2$ under nitrogen. The as-prepared sample was annealed in vacuum under different conditions. It appears that the annealing temperature dependences of the crystallite size, and photoluminescence and photostimulated luminescence follow simple power laws. The intensity of the photostimulated luminescence also depends on the annealing time due to the continued formation of F^{+}-centres whereas the photoluminescence remains approximately constant after 1 h. The maximum intensity of photostimulated luminescence is reached after annealing at 900 $^{\circ}$C for 4-6 h.

The present mechanochemical method with subsequent annealing has the potential to result in photostimulable phosphors with much higher sensitivity and spatial resolution. For example, we expect that the addition of a few percent of BaI$_2$ in the ball milling process will lead to higher sensitivity.

The photostimulated luminescence spectra of batches of nanocrystalline BaFBr:Eu^{2+} as a function of annealing time at 900 $^{\circ}$C are shown in Fig. 6, again compared to the commercial imaging plate. The increase of photostimulated luminescence intensity with annealing time follows a simple exponential law of the form

$$f(t) = A\left[1 - \exp(-kt)\right] \qquad (1)$$

with parameter values of A=531 (in a.u.) and k=0.89/h.
In particular, the intensity of the sample after annealing for 6 h is ~10 times higher than that of the commercial imaging plate. However, it was x-irradiated with a 10 times higher surface dose. In addition, the nanocrystalline BaFBr:Eu^{2+} samples were pressed into an aluminium sample holder with a depth of 500 μm, while the commercial film is ~80-100 μm thick. The sample used in our experiment is thus about 5× thicker than a

The ball milling preparation method with subsequent annealing at 400-900 ^{o}C may also allow the tailoring of the particle shape and size distribution in order to maximize the packing density.[25] This in turn may render higher sensitivities and also higher resolution in computed radiography due to the smaller particle size in comparison with the ~5 μm particles that are typically used in the preparation of commercial imaging plates. The ball milling method has also the advantage of yielding homogenous distributions of the elements on the atomic level.[26]

In conclusion, the present preparation route appears to be much more straightforward than currently used methods and potentially leads to more efficient BaFX:Eu^{2+} x-ray storage phosphors plates.

Acknowledgements

Notes and references

1   M. Sonoda, M. Takano, J. Miyahara and H. Kato, *Radiology.*, 1983, **148,** 833-838.
2   K. Takahashi, K. Kohda, J. Miyahara, Y. Kanemitsu, K. Amitani and S. Shionoya, *J. Lumin.*, 1984, **31–32**, 266-268.
3   K. Takahashi, J. Miyahara and Y. Shibahara, *J. Electrochem. Soc.*, 1985, **132**, 1492-1494.
4   H. von Seggern, *Braz. J. Phys.*, 1999, **29**, 254-268.
5   J. M. Spaeth, T. Hangleiter, F. K. Koschnick and T. Pawlik, *Radiat Eff. Defects Solids.,* 1995, **135**, 1-10.
6   S. Schweizer, *Phys. Status Solidi A.*, 2001, **187**, 335-393.
7   J. M. Spaeth, *Radiat. Meas.,* 2001, **33**, 527-532.
8   T. Hangleiter, F. Koschnick and J. Spaeth, *J. Phys: Condens. Mat.*, 1990, **2**, 6837-6846.
9   A. Meijerink and G. Blasse, *J. Phys. D: Appl. Phys.*, 1991, **24**, 626-632.
10 F. K. Koschnick, J. M. Spaeth, R. S. Eachus, W. G. McDugle and R. H. D. Nuttall, *Phys. Rev. Lett.*, 1991, **67**, 3571-3574.
11 R. S. Eachus, R. H. D. Nuttall, M. T. Olm, W. G. McDugle, F. K. Koschnick, T. Hangleiter and J. M. Spaeth, *Phys. Rev. B.*, 1995, **52**, 3941-3950.
12 M. Salis, *J. Lumin.*, 2003, **104**, 17-25.
13 R. J. Klee, *J. Phys. D: Appl. Phys.*, 1995, **28**, 2529-2533.
14 A. Meijerink, *Mater. Chem. Phys.*, 1996, **44**, 170-177.
15 S. Schweizer, J. M. Spaeth and T. J. Bastow, *J. Phys.:Condens. Matter.*, 1998, **10**, 9111-9122.
16 Q. Liang, Z. Li, W. Ma, Y. Shi and X. Yang, *Mater. Res. Bull.*, 2012, **47**, 2357-2363.
17 H. von Seggern, S. Hesse, J. Zimmermann, G. A. Appleby, X. Meng, C. Fasel and R. Riedel, *Radiat. Meas.*, 2010, **45**, 478–484.
18 Z. Liu, M. A. Stevens-Kalceff, X. Wang and H. Riesen, *Chem. Phys. Lett.*, 2013, **588**, 193-197.
19 X. Wang, Z. Liu, M. A. Stevens-Kalceff and H. Riesen, *Inorg. Chem.*, 2014, **53**, 8839-8841.
20 X. Wang, H. Riesen, M. A. Stevens-Kalceff and R. P. Rajan, *J. Phys. Chem. A.*, 2014, **118**, 9445–9450.
21 R. Kolb, M. Schlapp, S. Hesse, R. Schmechel, H. von Seggern, C. Fasel, R. Riedel, H. Ehrenberg and H. Fuess, *J. Phys. D: Appl. Phys.*, 2002, **35**, 1914-1918.
22 H. Hagemann, F. Kubel and H. Bill, *Mater. Res. Bull.*, 1993, **28**, 353-362.
23 G. K. Williamson and W. H. Hall, *Acta. Metall.*, 1953, **1**, 22–31.
24 Q. Ju, Y. Liu, R. Li, L. Liu, W. Luo and X. Chen, *J. Phys. Chem. C*, 2009, **113**, 2309-2315.
25 H.Y. Sohn and C. Moreland, *Can. J. Chem. Eng.,* 1968, **46**, 162-167.
26 L.J. Yin, W.W. Hu, X. Xu and L.Y. Hao, *Ceram. Int.*, 2013, **39**, 2601-2604.